IOP Conf. Series: Materials Science and Engineering **730** (2020) 012020 doi:10.1088/1757-899X/730/1/012020

Fracture Analysis of the Chain Pin Shaft of an Escalator Ladder

Chenghong Peng[1,*], Weiheng Zhu, Ling Chen, Xiaoke Zhu and Zhiling Chen

School of Materials Science and Engineering, South China University of Technology, Guangzhou 510641, China
*mehpeng@scut.edu.cn

Abstract. This study analyzed the cause of fracture for the chain pin shaft of an escalator ladder, and found that the pin material satisfied the chemical composition content requirements of the GB 20CrMo steel standard and similar to ASTM A29/A29M-2012 grade 4120. Abnormal metallurgical quality defects were not found in the pin. The pin shaft was carburized, and internal oxidation defects were not observed on the surface as a result of carburization. The internal structure of the material was uneven, there existed a mixed grain structure, and the martensite structure was coarse at particular regions, to seven grade. Additionally, the martensite structure in the carburized layer was slightly coarser, four to five grade, which had an adverse effect on the pin strength. The pin break was a fatigue fracture caused by multiple cumulative damages. The fracture originated on the surface of the pin, and may have been caused by indentation on the pin's surface.

1. Introduction

Escalator accidents occasionally occur; minor accidents cause property damage, while serious accidents result in human casualties. Determining the cause of such accidents is very important for avoiding escalator accidents. By investigating a particular escalator accident, it was found that the chain pin shaft had broken. The appearance of the broken pin shaft is shown in figure 1. As can be seen in the figure, the pin break occurred on a smooth surface at a distance of approximately 4 mm from the R position of the variable cross-sections. The fracture surface was relatively flat and approximately perpendicular to the axial direction. There existed significant bruising at the edge of the fracture near the end of the larger diameter, as indicated by the arrow in figure 1(b).

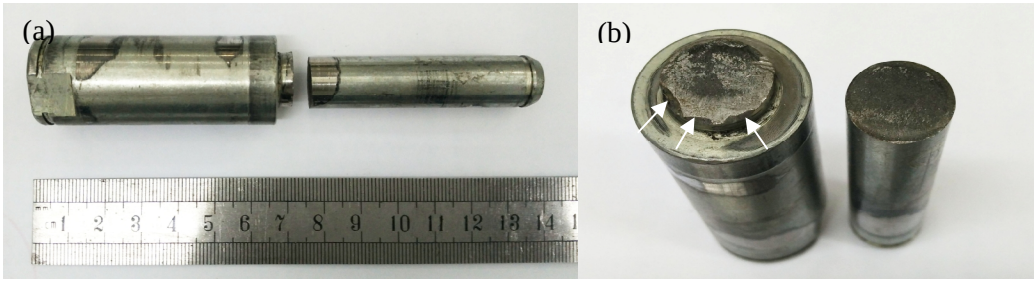

Figure 1. Appearance of stepped pin shaft fracture: (a) overall appearance of broken part of step chain pin; (b) macroscopic morphology of uncleaned fracture.

The total length of the step chain was approximately 135 mm; the larger end diameter was approximately Φ25×66 mm, and the smaller one was approximately Φ15×69 mm. The pin was made

of 20CrMo steel and used in the automatic walking elevator step chain; the surface hardness requirement was 56-60 HRC. In this study, fracture analysis, material chemical composition analysis, material metallographic analysis, and mechanical property testing were carried out to determine the main cause of the pin shaft fracture.

2. Experimental Procedure

The failure shaft was visually and macroscopically inspected by optical microscopy and chemical analysis. The hardness was also measured to complete the characterization of the materials. The chemical analysis was carried out using FOUNDARY MASTER desktop vacuum spark emission spectroscopy. The fractured surfaces were ultrasonically cleaned and observed using a scanning electron microscope (SEM) equipped with Energy Dispersive X-Ray Spectrometer (EDX).

Metallographic observation was carried out using the Leica DMI5000M microscope. The sample was etched using 4% nitric acid alcohol solution.

3. Fracture Macro- And Micro-Analysis

3.1. Macro Analysis

The macroscopic morphology of the broken shaft fracture after cleaning is shown in figure 2, the main cracking source of the broken shaft was located on the surface of the shaft, and a secondary cracking source was observed near the shaft surface in the fracture. The expansion direction of the main crack is indicated by the red arrows in the figures. Moreover, there existed a faint beach-like pattern on the fracture, which indicated that the pin fracture may have been fatigue fracture.

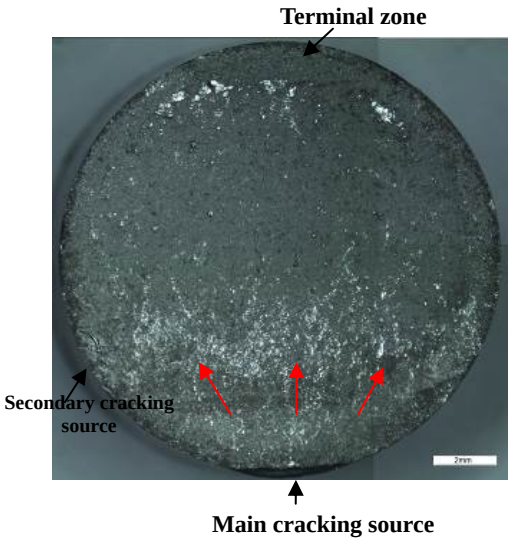

Figure 2. Low optical magnification fracture image of broken shaft fracture after cleaning.

3.2. Microscopic Analysis

The microtopography of the broken shaft fracture is shown in figure 3-1(a)-(b), there is a trace of collision in the main cracking source, which may have been formed after the pin broke. Therefore, it is impossible to confirm whether the cracking source cracked owing to metallurgical quality defects or processing defects. This fracture near the surface of the shaft was mainly intergranular brittle fracture, which indicates that the material of the shaft surface was brittle.

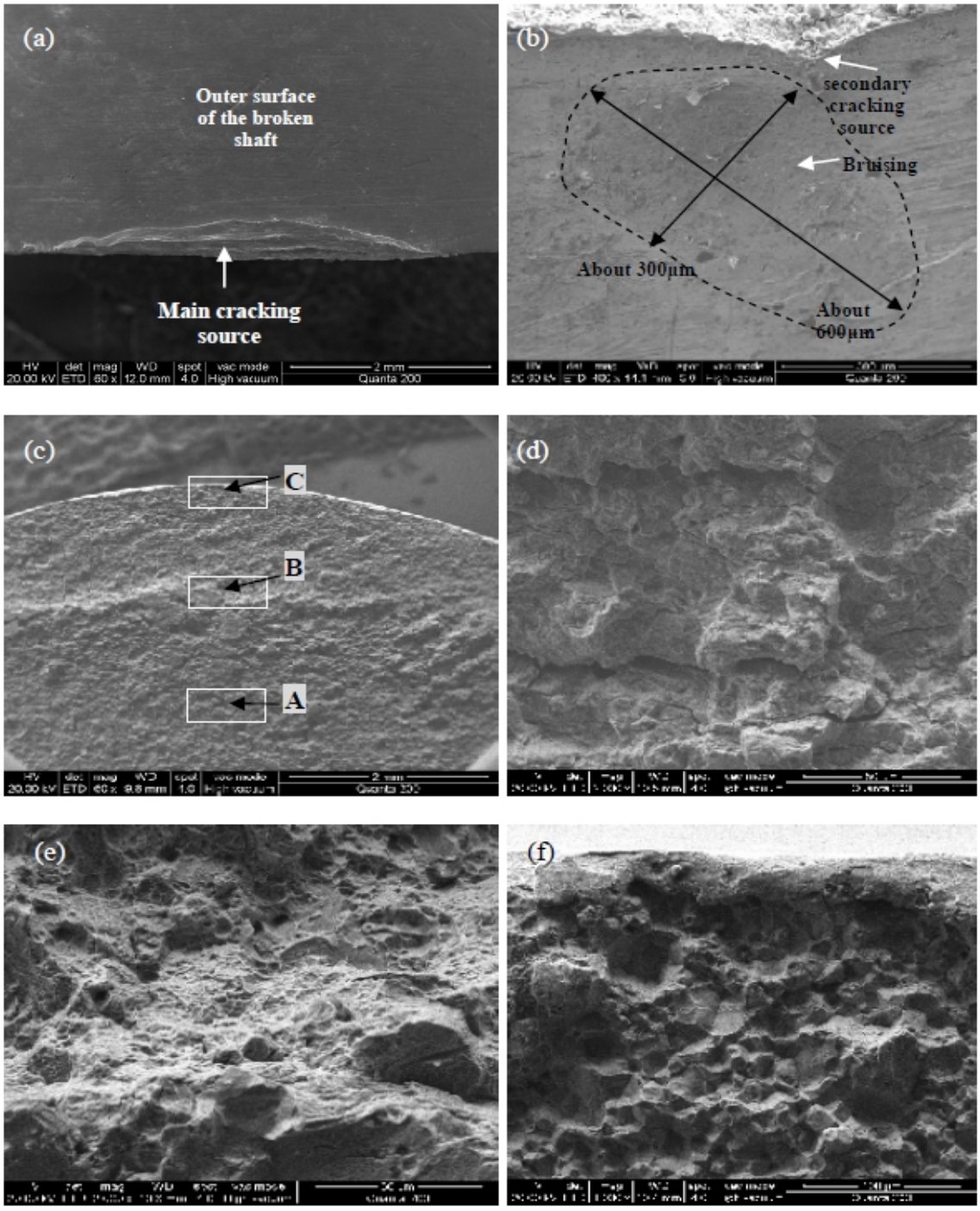

Figure 3-1. Microscopic morphology of broken shaft fracture. (a) Main crack source area shown in figure 2; (b) Outer surface close to secondary crack source; (c) Near termination zone shown in figure 2; (d) Area A in (c) (fatigue striation); (e) Area B in (c) (dimple); (f) Area C in (c) (brittle intercrystalline fracture in rock candy form).

In figure 3-1(c)-(d), in addition to the main cracking source, a secondary cracking source can be observed in the vicinity of the main cracking source. Abnormal metallurgical quality defects were not observed in the secondary cracking source region of the fracture, but a bruise mark was observed on the pin surface near the secondary cracking source region. The size of the crushed part was approximately 600×300 μm. Considering the small probability of only forming such a small crush at

the secondary cracking source after the pin broke, it is believed that the crush mark formed before the fracture and caused the creation of the cracking source.

In figure 3-1(e)-(f), there existed a fatigue striation on the fracture, which indicated fatigue fracture. Thus, the fracture of the pin was actually fatigue fracture in the termination zone belonging to the instantaneous fracture zone, and the microscopic features of the fracture near the core were mainly dimples. Additionally, the microscopic features of the fracture near the surface area mainly indicated a brittle intercrystalline fracture in the form of rock candy. This indicates that the pin was subjected to surface strengthening treatment, and thus the core material had good toughness.

In summary, the pin fracture was fatigue fracture, but the main fatigue source was damage by crushing after the pin broke. Therefore, it was impossible to confirm the crack source defect that caused the pin to undergo fatigue fracture by the secondary crack source; namely, the pin surface pressure injury defects. Hence, it was assumed that the main cracking source may also had similar crushing defects resulting in fatigue cracking.

3.3. Material Chemical Composition Testing

The chemical composition of the sample was detected by desktop vacuum spark emission spectroscopy according to ASTM E415-2017. The test results of the chemical composition of the investigated broken shaft material are presented in table 1.

Table 1. Results of broken shaft material's chemical composition analysis.

Material	chemical composition (wt. %)								
	C	Si	Mn	P	S	Cr	Mo	Cu	Ni
Measured value	0.20	0.26	0.62	0.018	0.009	1.08	0.20	0.041	0.026
GB 20CrMo	0.17~ 0.24	0.17~ 0.37	0.40~ 0.70	*	*	0.80~ 1.10	0.15~ 0.25	*	≤ 0.30
ASTM A29/A29M 4120	0.18~ 0.23	0.15~ 0.35	0.90~ 1.20	<0.035	<0.040	0.40~ 0.60	0.13~ 0.20		

According to the chemical composition analysis results, the chemical composition of the broken shaft material satisfied the requirements regarding the standard component content of the "China GB standard 20CrMo steel", and indicated special-grade high quality steel. The chemical compositions are similar to those of the ASTM A29/A29M-2016, grade 4120 also.

3.4. Metallographic Analysis of Materials

According to ASTM E3-11 (2017), the axial and radial metallographic analysis specimens were collected near the cracking source area at the end of the smaller diameter of the broken shaft to carry out metallurgical quality analysis and microstructural analysis.

The microstructure of the non-etched metallographic grinding surface of the axial specimen was observed. The non-metallic inclusion grade assessment according to ISO 4967-2013 results are presented in Table 2.

Table 2. Non-metallic inclusion rating.

Assessment project	Group A (sulfide type)		Group B (aluminate type)		Group C (silicate type)		Group D (globular oxide type)		Group DS (single globular type)
	Fine series	Thick series	Fine series	Thick series	Fine series	Thick series	Fine series	Thick series	
Grade	0	0	1.0	0	0	0	1.0	0	0

The non-metallic inclusions of the inspection materials were mainly "point type + chain type" oxide-based non-metallic inclusions. The degree of non-metallic inclusions in the material was not

severe, and abnormal metallurgical quality defects were not observed in the material. At the same time, internal oxidation defects resulting from carburization were not observed on the surface of the pin shaft.

The metallographic structure of the material was evaluated according to "GB/T 25744-2010 Metallographic examination for carburizing quenching and tempering of steel parts".

The microstructure of the axial surface of the axial specimen after etching is shown in figure 3-2, the microstructure image of the radial surface after etching the specimen is shown in figure 3-3. The microstructure of the material indicates that the surface of the broken shaft was carburized. The tempered martensite structure of the carburized layer was slightly coarser, four to five grade, which led to an increase in the brittleness of the shaft surface material. Moreover, the grain of the pin matrix material was uneven, and there existed an abnormally coarse tempered martensite microstructure in particular regions. The hardness of the coarse grain zone determined using the Micro Vickers hardness method was 430-460 HV, and the hardness of the fine grain zone was 360-380 HV. The mixed grain microstructure had a negative effect on the strength of the material[1, 2, 3, 4]. Because the sample to be inspected was very small, tensile testing and impact testing could not be performed.

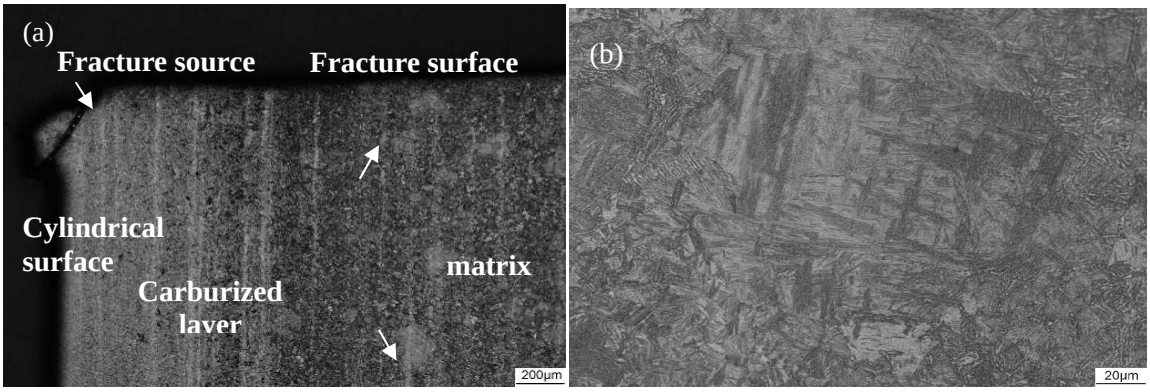

Figure 3-2. Microstructural morphology of axial matrix specimen near outer surface in cracking source area: (a)Low-magnification morphology (arrow on matrix indicates coarse martensite area); (b) High-magnification morphology of coarse-grained matrix region, light block area in (a).

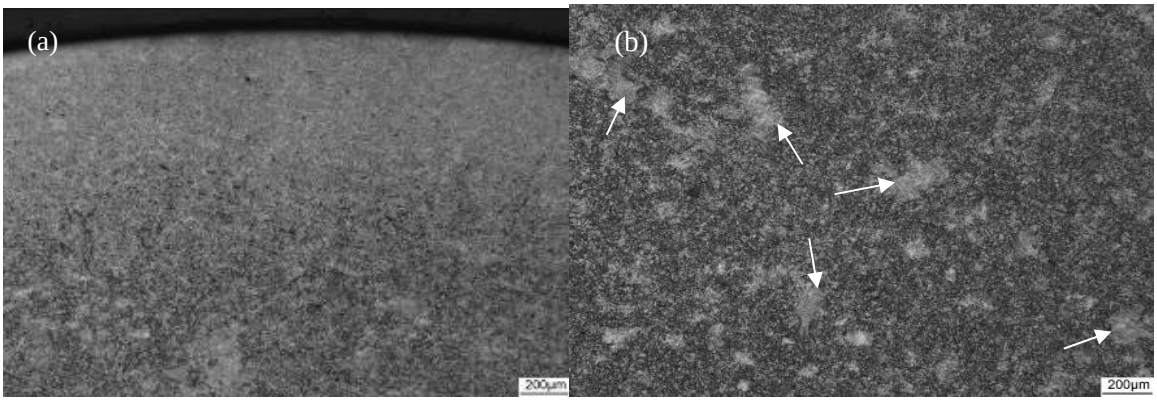

Figure 3-3. Microstructural morphology of radial matrix specimen: (a) near surface; (b) close to core (arrow indicates coarse martensite area).

According to the Chinese machinery industry standard "JB/T 9211-2008 Martensite grade medium-carbon steel medium-carbon alloy structural steel", the tempered martensite structure grade to base in the coarse grain zone was assessed as 7 grade, and the tempered martensite grade in the fine grain zone was 4 grade. A mixed grain structure appeared inside the material, maybe owing to the abnormal growth of local grain resulting from the short duration of over-temperature during the heat

treatment of the material. Alternatively, it may have occurred owing to improper forging also, such as the forging ratio may have been insufficient , or the final forging temperature may have been too high, or uneven temperature, thus resulting in an uneven material structure and partial coarse grain regions[5,6,7]. Additionally, the mixed grain structure was more likely to occur under normal heat treatment conditions; grain refining by micro-alloying was effective in suppressing the formation of mixed grain[8].

The mixed grain of carburized steel and quenched and tempered steel was investigated under normal heat treatment conditions. A simulation test was carried out using cylindrical samples with a size of approximately 12 mm×12 mm, whose original microstructure was a normal annealed state. Thus, it was observed that in the process of heat treatment, low-carbon steels, such as 20Cr, 20CrMo, and 20CrMnTi, were prone to the occurrence of abnormally coarse grain in local areas. Some hold that mixed grain is produced after heat treatment. However, it is not a heat treatment defect, but rather a defect in the steel itself, such as uneven deformation or uneven composition.[7]

Energy spectrum analysis confirmed that there existed a coating with a thickness of approximately 1 μm as a galvanized layer on the shaft surface (figure 3-4). From the appearance of the coating distribution in the fracture source region and the deformation of the structure, it was assessed that the region formed by collision after the pin broke.

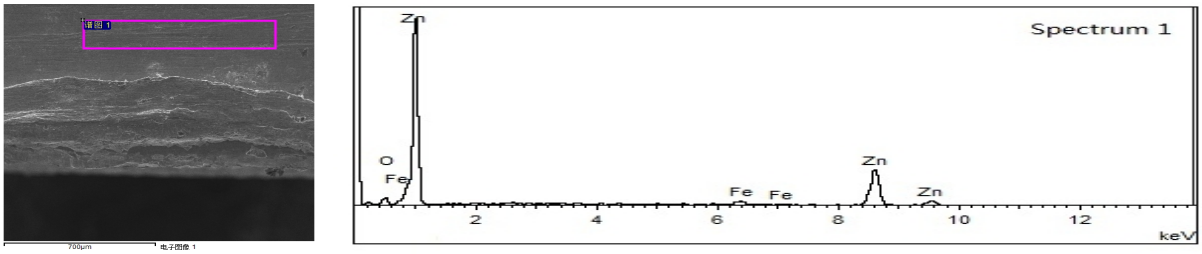

Figure 3-4. Energy spectrum analysis results for coating on pin surface.

4. Micro-Hardness Test

Because the sample was too small, impact and tensile tests could not be performed. According to the ASTM E18-2019, Surface and core Rockwell hardness test was performed on the broken shaft surface and the core, their average hardness in 56.6 and 35.0HRC.

According to the test results, the surface hardness of the broken shaft achieved the required hardness value (56-60 HRC) provided by the client.

The hardness distribution of the hardened layer on the surface of the pin shaft was tested according to "ASTM E92–17 Standard Test Methods for Vickers Hardness and Knoop Hardness of Metallic Materials" and "ISO 2639-2002 steels–determination and verification of the depth of carburized and hardened cases". The detection location of the broken shaft was on the cross-section of the pin shaft with a thin end and a distance of approximately 10 mm from the fracture surface. The test results are presented in figure 4.

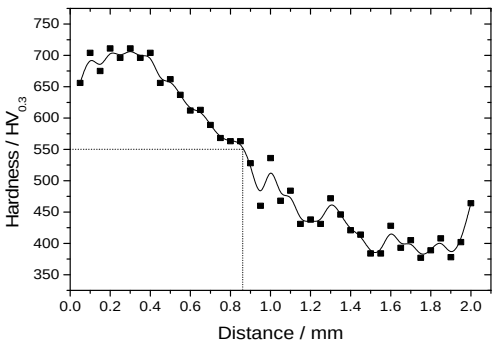

Figure 4. Hardness distribution curve of hardened layer on broken shaft.

The surface hardness change of the broken shaft conforms to the general rule of hardness change after carburizing treatment, as can be seen, the effectively hardened layer depth of the broken shaft was approximately 0.86 mm, according to ISO 2639-2002. And the hardness of the matrix fluctuates greatly, further indicating that the microstructure of the matrix is uneven.

5. Conclusion

(1) The chemical composition of the pin material satisfies the chemical composition content requirements of 20CrMo steel according to the "GB/T 3077-2015 alloy structural steels" standard, which similar to "ASTM A29/A29M-2012 Standard Specification for Steel Bars, Carbon and Alloy, Hot-Wrought, General Requirements for grade 4120". Abnormal metallurgical quality defects were not observed in the pin.

(2) The internal structure of the material was uneven, a mixed grain structure was observed, and the martensite structure was coarse in particular regions (7 grade), while the martensite structure in the layer was slightly coarser (four to five grade), which had an adverse effect on the pin strength. Hence, the material's strength decreased.

(3) The pin break was fatigue fracture caused by cumulative damage. The fracture originated on the surface of the pin, and may have been caused by indentation on the pin's surface.

6. Acknowledgment

We thank Experimental Center of Materials Science and Technology, SCUT, for composition analyses and SEM observation on the chain pin shaft.

7. References

[1] Wang Kai, Dang Shu'e, He Yan, Liu Zhilong 2013 Methods of Eliminating Mixed Grains in 30Cr2Ni4MoV Steel, *Heavy Casting and Forging* **6** 9
[2] Feng Shihuan Liang Huidong 2011 Research on Formation Causes of Mixed Austenite Grain in 20Cr Steel, *Metallurgical Collections* **8** 1
[3] Tian Xiugang, Feng Xianyong, Song Xiaojuan 2018 Analysis and Control of Surface Mixed Crystal in Ultra- Low Carbon Hot Strip Steel, *Hebei Metallurg* **6** 47
[4] Anders From and Rolf Sandström 1999 Influence of Mixed Grain Size Distributions on the Toughness in High and Extra High Strength Steels, *Materials Characterization* **42** 111
[5] SHEN Qunfang, WU Shaobin 2011 20CrMnTi"MixGrain"Analysis, Modern machinery **3** 90
[6] Zhinan Yang, Fucheng Zhang, Chunlei Zheng , Ming Zhang , Bo Lv, Lin Qu 2015 Study on hot deformation behaviour and processing maps of low carbon bainitic steel, *Materials and Design* **66** 258
[7] Song Haigang 2018 Reasons for mixing crystals of F91 steel and elimination methods, *China Metal Bulletin* **8** 71
[8] Zhu Hua 2017 Analysis of Reasons for Formation of Mixed Grain in Carburized Gear Steel 18CrMnB with Different Heat Treatment Processes, *Special Steel Technology* **2** 40